Journal of Research and Applications in Mechanical Engineering
ISSN: 2229-2152 (Print); 2697-424x (Online)
(2023) Vol. 11, No. 2, Paper No. JRAME-23-11-012
[DOI: 10.14456/jrame.2023.12]

Research Article

Numerical Study of Channel Structure Effects on Thermal Hydraulic Performance of Printed Circuit Heat Exchanger

N. Nyein Aye
C. Thumthae*
W. Hemsuwan
School of Mechanical Engineering, Suranaree University of Technology, Nakhon Ratchasima 30000, Thailand

Received 20 January 2023
Revised 16 March 2023
Accepted 8 May 2023

Abstract:
Printed circuit heat exchangers (PCHEs) enable high efficiency, high pressure resistance, highly compact geometry, a better heat transfer coefficient, and the ability to withstand a large operating temperature range. The current study aims to analyze their comprehensive performance based on numerical methods, and reliable heat transfer is required to operate at high pressures and high applications. A three-dimensional single-banking PCHE was designed in the computational fluid dynamics (CFD) software Fluent. First, the effects of zigzag and straight channels on the PCHE's performance along with the pressure drop and heat transfer characteristics were investigated. The zigzag channel showed a higher comprehensive performance up to 22% than the straight channel. Second, a different zigzag channel diameter range (2 mm – 4 mm) and their effects on the PCHE's performance were analyzed. A small-channel diameter of 2 mm reduced the pressure drop and increased heat transfer. This work was aimed at determining a better flow channel structure to improve thermal-hydraulic performance.

Keywords: *Zigzag-channel, Straight-channel, Channel-diameter, Pressure drop and heat-transfer, Thermal-hydraulic performance*

1. Introduction

Printed circuit heat exchangers (PCHEs) are promising intermediate heat exchangers. It has a high heat-transfer performance, high efficiency and a high-integrity structure. Moreover, they can be applied over a wide range of temperatures and pressures [1]. The photochemical etching technique was used for a very small channel diameter (microchannel), and the etched plates were bonded together using the diffusion method. The resulting PCHEs possess exceptional strength and integrity owing to the absence of joints, welds, or points of failure. The PCHEs weight can be reduced by approximately 1/30 of that of conventional heat exchangers, such as shell-and-tube heat exchangers, under the same heat duty [2]. Therefore, PCHEs are suitable for various engineering applications such as cryogenic applications, supercritical fluid Brayton cycles, and nuclear power generation.

According to the flow path, PCHE can be divided into two types: continuous and discontinuous. The continuous channels are straight, zigzag, and wavy, and the discontinuous channels include S-shaped and airfoil fins [3]. In recent years, the heat transfers and hydraulic characteristics of the PCHE thermal basis design have been numerically and experimentally investigated. The zigzag channel PCHE was both numerically and experimentally investigated by Chen et al. [4] for the dynamic response model. Helium was used as the working fluid. The results showed the reliability of the dynamic model based on a comparison of the simulation and experimental data.

* Corresponding author: C. Thumthae
E-mail address: chalothorn@sut.ac.th

A geometrical structure simulation of the airfoil-fin PCHE was performed by Chu et al. [5]. The dynamic performance and heat-transfer characteristics were determined using various pitch simulations. In addition, they proposed dimensionless correlations of the *j* factor for the heat transfer and *f* factors for pressure losses. Some researchers [6, 7] numerically investigated the effect of zigzag channel bending angles on heat-transfer performance. They found that a bending angle of 45˚ increased the heat-transfer and pressure drop. Chu et al. [8] analyzed the straight-channel PCHE performance. Supercritical carbon dioxide (sCO_2) and water heat-transfer platform were used. They discovered that the sCO_2 heat-transfer performance was greater about 1.2–1.5 times than that of water. Zhang et al. [9] numerically analyzed the thermal characteristics of a straight-channel PCHE using a natural-gas phase. Zhao et al. [10] analyzed the effects of the zigzag channel performance based on various bend angle, mass flux, and inlet pressure. A region lower than the 15˚ bend angle exhibited better heat-transfer performance during the range of mass flux from 207.2 to 621.6 kg/m^2.s, and an increase in inlet pressure reduced the pressure drop. The effect of a narrow cross-section wavy channel on the PCHE thermal-hydraulic performance was numerically studied by Yang et al. [11]. The narrow cross-section channel slightly dropped the total heat transfer rate and increased the pumping power. Lee et al. [12] investigated the effect of channel cross sections (semicircular, rectangular, trapezoidal and circular) on thermal-hydraulic performance. Jeon et al. [13] analyzed the thermal performances of cross-sectional shape channels, namely semicircular, triangular, rectangular, and elliptical, using the numerical method. The results showed that the channel cross-sectional shape had no significant influence on the thermal performance because the hydraulic diameter remained the same. Wang et al. [14] compared the thermal and hydraulic performances of straight-type PCHEs with circular and different widths of rectangular channels. At the same mass flux simulation, the increase in rectangular channel width can significantly influence the heat transfer rate per unit volume and decrease the pressure drop.

The PCHE heat transfer enhancement can increase the convective heat transfer coefficient or the surface heated area. The zigzag channel PCHE extends the heated surface area and provides a better heat transfer performance between the primary and secondary working fluids. Seung et al. [15] proved that zigzag channel PCHE for helium-helium application is a better configuration under laminar flow conditions. This is because of the low-pressure drop and high heat-transfer area. Therefore, this study interested on zigzag channel PCHE. The literature research conditions from the above study revealed the influence of channel structures on the thermal-hydraulic performance of PCHE. Therefore, the first objective of the present study was to investigate the effect of the channel shape on the thermal-hydraulic performance of PCHE. The zigzag and straight channels were applied. In zigzag channel analysis, most studies focused on the influence of bend angle and mass flux. Similarly, some studies found that the cross-section channel shape has great influence on thermal and hydraulic performance. However, all studies compared the effect of channel shapes on thermal and hydraulic performance. Therefore, it is still needed to further study of channel cross-section effect on PCHEs performance. The second objective of the present research was to analyze the appropriate semicircular zigzag channel diameter that provides the best performance for the printed circuit heat exchanger.

2. Methodology

2.1 Description of Numerical Physical and Boundary Condition

For the numerical model, Chen et al. [16] 15˚ zigzag channels with round corners (fillet radius = 4 mm) and straight channel used. For simulation, Ansys fluent commercial software was used. The counter-flow channels with a cross-section are shown in Fig. 1. The cold side is blue, the hot side is red, and the solid material is shown in gray in Figs. 1(a) and (b). To reduce computational resources and time [17], a numerical model was set up as a single banking method. The top, bottom, left, and right positions were set as the periodic boundary conditions. The entire channel length was divided into 8.5 pitches. A pitch length (*P*) was 24.6 mm. For the simulation, the numerical models were set to the steady-state condition, inlet mass flow rate, and pressure outlet. The inlet temperatures on the cold and hot sides were 350˚C and 800˚C, respectively, and the outlet and working pressures were 3 MPa on both sides. Supercritical helium was used as working fluid. The thermal-physical of helium properties depend on temperature and pressure and have been imported from the NIST chemistry webbook [18]. The solid material was Alloy 617 with a density of 8360 kg/m^3, and its properties changed with the temperature obtained from Special Metals [19].

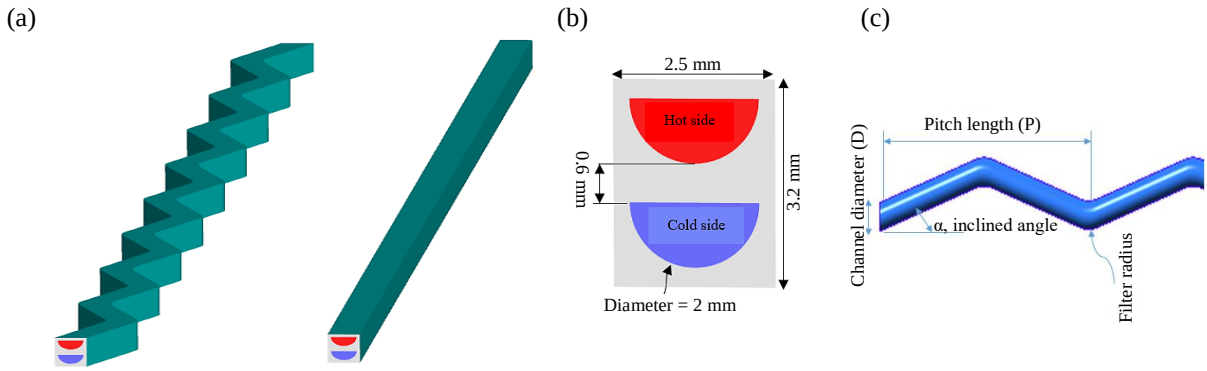

Fig. 1. (a) 3D models of zigzag and straight channels. (b) Cross-sectional view of simulation domain. (c) Span wise direction of the zigzag pitches.

2.2 Simulation Method and Data Reduction

The ANSYS Fluent commercial software was used to perform the simulation. The average Reynolds number (*Re*) range was considered lower than 2300. Therefore, the simulation employed steady state and laminar model. For the coupling of velocity and pressure, the simple algorithm was set up. This is because the small error between the SIMPLE algorithm simulation and experimental data compared with the other algorithms. Moreover, SIMPLE algorithm saves the memory than Coupled algorithm. To solve the momentum and energy, a second-order upwind scheme was used for accurate results. In simulation, viscous dissipation and thermal radiation effects were not considered. The governing equations of continuity, momentum and energy for the fluid flow and heat transfer are (1) - (3) [20]:

$$\nabla . U = 0 \tag{1}$$

$$U . \nabla (\rho U) = -\nabla p + \nabla . (\mu . \nabla U) \tag{2}$$

$$U . \nabla (\rho C_p T_f) = \nabla . (k_f \nabla T_f) \tag{3}$$

In the governing equations: ρ, U, μ, k, T, C_p represent the density of the fluid, the velocity, viscosity, thermal conductivity, temperature, and specific heat.

For global data analysis, the performance of pressure drop and the heat transfer are defined as follows [16]:

$$\Delta P = P_{inlet} - P_{outlet} \tag{4}$$

$$\text{Convective heat-transfer coefficient} = h = \frac{q''}{\left| T_f - T_w \right|} \tag{5}$$

$$T_f = \frac{(T_{inlet} + T_{outlet})}{2} \tag{6}$$

$$T_w = \frac{(T_{h,inlet} + T_{h,outlet} + T_{c,inlet} + T_{c,outlet})}{4} \tag{7}$$

where P_{outlet} and P_{inlet} are the average inlet and outlet pressure, respectively. T_w is the temperature at wall, and T_f is the fluid temperature, q'' is the constant wall heat flux. Cold side is denoted as *c* and hot side as *h*, *f* as bulk fluid.

$$\text{Nusselt number} = Nu = \frac{hD_h}{k} \tag{8}$$

$$\text{Hydraulic diameter} = D_h = 4A/p \tag{9}$$

$$\text{Fanning friction coefficient} = f = \frac{\Delta P_f \, D_h \, \bar{\rho} \, A_c^2}{2l\dot{m}^2} \tag{10}$$

where the thermal conductivity symbol as k, A_c is the cross-sectional area. l is the actual channel flow length, and $\bar{\rho}$ is bulk fluid density. For local analysis,

$$h_i = \frac{q''_{w,i}}{T_{w,i} - \frac{(T_{inlet,i} + T_{outlet,i})}{2}} \tag{11}$$

where the subscript i represents for the ith segment, the local convective heat-transfer coefficient defined as h_i, the local heat flux is $q''_{w,i}$. $T_{w,i}$ is the averaged wall surface temperature that is in contact with the surrounding fluid, $T_{inlet,i}$ and $T_{outlet,i}$ are at local inlet and outlet temperature, respectively.

2.3 Grid Independence and Model Validation

Table 1: Mesh grid independency simulation results.

Mesh (million)	T_{outlet} **(K)**		ΔP **(kPa)**	
	Cold side	**Hot side**	**Cold side**	**Hot side**
0.124	938.22	757.62	14747.7	15384.8
1.95	954.36	740.06	15324.5	16091.5
3.123	947.10	748.80	15947	16578.1
4.87	948.78	747.00	15350	16000

As shown in Table 1, four mesh-grid elements were studied: 0.124, 1.95, 3.123, and 4.87 million. The mesh grids were generated in the ANSYS Mesh software. For the mesh-independence study, an inlet mass flow rate of approximately 9.7857×10^{-5} kg/s per channel in both channels was simulated. The outlet temperature and pressure drop were measured. To determine the appropriate mesh grid, the fine mesh results were used to calculate the relative error [7] in Equation (12). In comparison, a grid number of 0.124 million showed about up to 3.924% on pressure drop and 1.422% an outlet temperature with the fine mesh results. When the mesh grid number was greater than 1.95 million, the maximum relative error was approximately 0.928% for the outlet temperature and 3.889% for the pressure drop, which is the safety percentage error. Therefore, a grid number of 1.95 million was suitable for saving computational time and obtaining accurate results. The structured meshes for the computational domain are shown in Fig. 2. For model validation, the Reynolds number test was simulated, and validated using the results of Chen et al. [16]. The validation is shown in Fig. 3. The present simulation has some discrepancies of up to 5% with Chen et al.'s simulation, 31% with the experimental results for the Fanning friction factor, and 10% and 2% for the Nusselt number. Thus, the zigzag channel PCHE model was strongly validated for use in numerical studies.

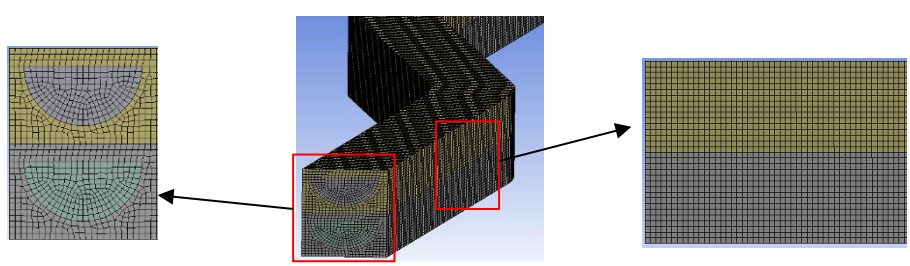

Fig. 2. 1.95 million Mesh generation of computation domain.

$$Error(\%) = \frac{\left| Based \quad data \quad - \quad Measured \quad data \right|}{Based \quad data} \times 100\% \tag{12}$$

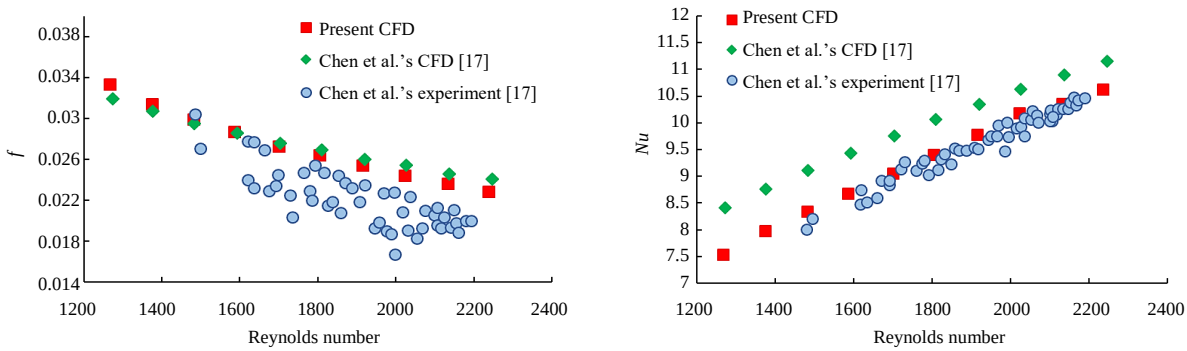

Fig. 3. Global Fanning friction factor (*f*) comparison, and global Nusselt number (*Nu*) comparison.

3. Results and Discussion

3.1 Relation between Channel Structure and Thermo-Physical properties

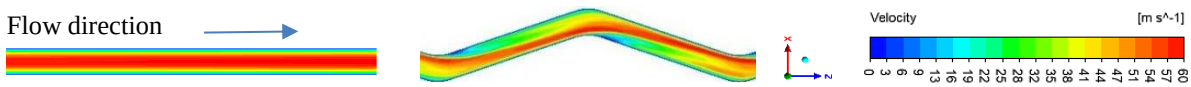

Fig. 4. Velocity distribution of straight and zigzag channels at pitch number (N = 8).

Fig. 5. Temperature distribution of straight and zigzag channels at pitch number (N = 8).

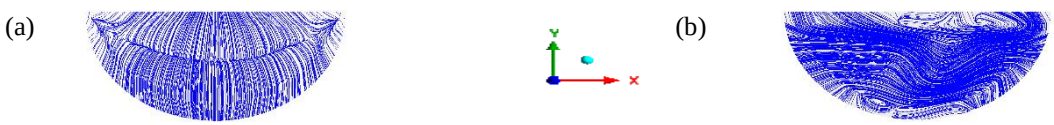

Fig. 6. Streamlines distribution at a pitch number (N = 8) (a) straight and (b) zigzag channel.

The variation of thermo-physical properties depending on channel structure was studied at mass flow rate 8.515×10^{-5} kg/s simulation. In order to focus on the channel structure's effect, the channel's full length was considered equal pitch length (8.5 pitches) and the same inlet mass flowrate on both sides. The variation absolute velocity in the cold channels are shown in Fig. 4. It was found that the straight channel was no flow disturbance since it didn't have a bend corner. However, the zigzag channel exhibited flow separation around the corner. The flow moved from the inner curvature to the outer curvature of the wall. The flow curvature induced an intensive centrifugal force that created the flow separation. In addition, at the inner wall, a reverse pressure gradient is generated, leading to the holding of the secondary flow zone, creating a vortex and increasing the pressure drop [21].

As shown in Fig. 5, the temperature distribution in all channels increases from the wall to the fluid over the flow distance. The temperature distribution of the zigzag channel exhibited more significant variation than that of the straight channel. These results indicate that the curvature channel significantly influences the heat transfer. The flow channel asymmetry can be attributed to local heat flux changes after passing through a corner [22]. Therefore, the temperature distribution of the zigzag channel was not uniform. Figure 6 shows the streamline distribution at corner of the pitch number (N= 8). The straight channel exhibited no vortices resulting from the absence of a flow disturbance. In the zigzag channel, vortices are produced at the bending point. This is because the flow disturbance

at the outer wall was separated from that at the inner wall. A secondary flow is generated by the flow separation, which significantly enhances the heat transfer, mixing fluid, and accelerating core displacement [7]. These secondary flows indicate efficient cross-sectional fluid mixing, non-uniform temperature profiles, and a high heat-transfer rate.

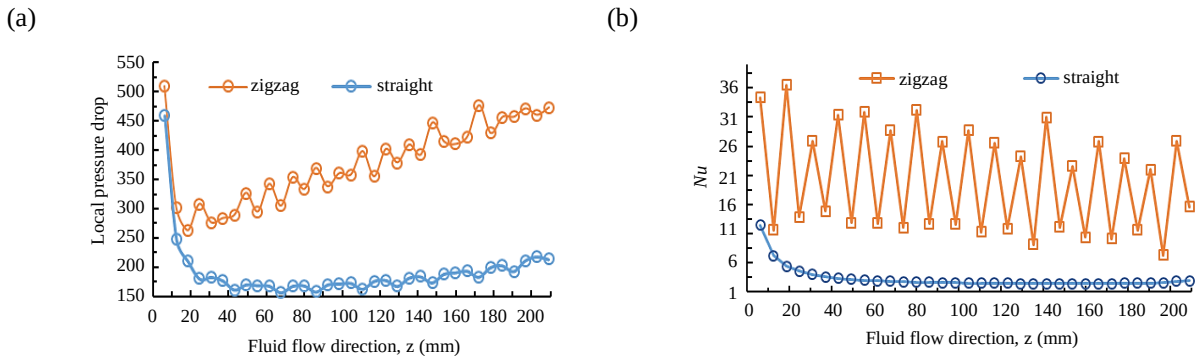

Fig. 7. (a) Local pressure drop and (b) local Nusselt number along flow direction.

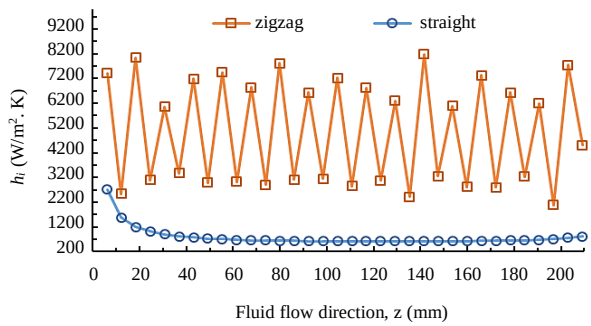

Fig. 8. Local convective heat transfer coefficient along the flow direction.

As shown in Fig. 7(a), the zigzag channel exhibited a higher pressure drop than the straight channel. The secondary flow in the zigzag channel was significant, as shown in Figs. 4 and 6, which led to an increase in pressure drop. The long length of the flow path also increased in the pressure drop. In Fig. 8, the zigzag channel has a higher heat transfer coefficient than the straight channel over the flow distance, resulting from the high heat-transfer rate (Fig. 5) and the actual flow area. The result of secondary flows with large vorticity structures (Figs. 6 and 4) significantly affects the fluid mixing and convective high heat-transfer rates. Therefore, the zigzag channel showed a significant heat transfer coefficient. Figure 7(b) shows the local Nusselt number (*Nu*), which is similar to the convective heat-transfer coefficient. The Nusselt number of the zigzag channel was larger than that of the straight channel. Because of the higher thermal energy transported by the hot surface, the viscosity and thermal conductivity were lower, the thinned film thickness and the higher convective heat-transfer coefficient, leading to a larger local *Nu*. As shown in Fig. 9, the local heat flux of the zigzag channel appears obviously non-uniform on the wall and significantly increased on the windward side of the channel corner. It is because incoming mainstream impacts on the windward sides and changes the flow direction, which leads to shifting the high heat flux zone and fluctuating the local Nusselts number.

3.2 Mass Flow Rate Effect on the Channels

From the mass flow rate 8.515×10^{-5} kg/s simulation, the channel shapes significantly affected the local flow and thermal performance. Therefore, the mass flow rate is one of an important parameter for analysis of PCHE performance. A different mass flow rate from 5.108×10^{-5} kg/s to 8.515×10^{-5} was applied to the global thermal-hydraulic performance of PCHE analysis.

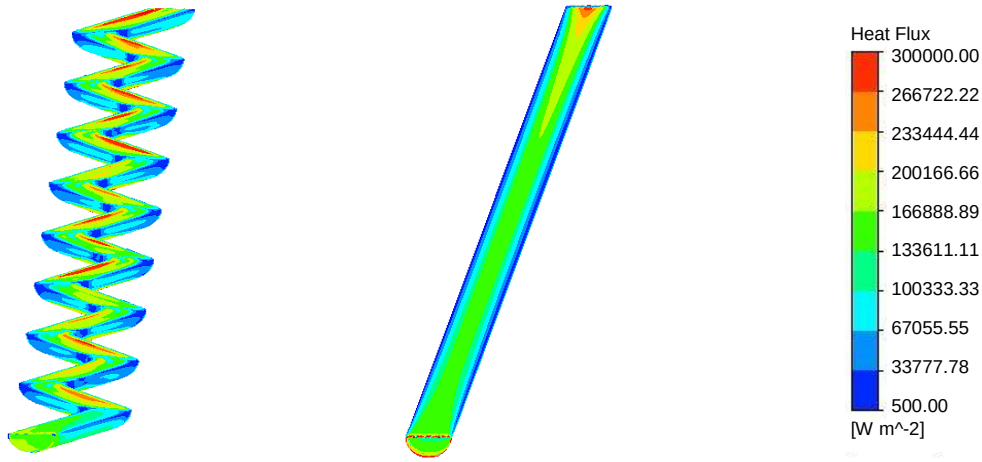

Fig. 9. Local heat flux of the zigzag channel and straight channel

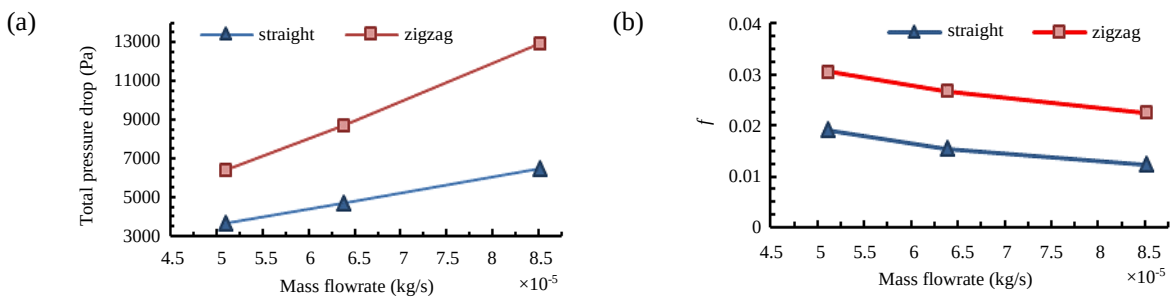

Fig. 10. (a) Total global pressure drop, and (b) global Fanning friction factor at different mass flow rates for different channels.

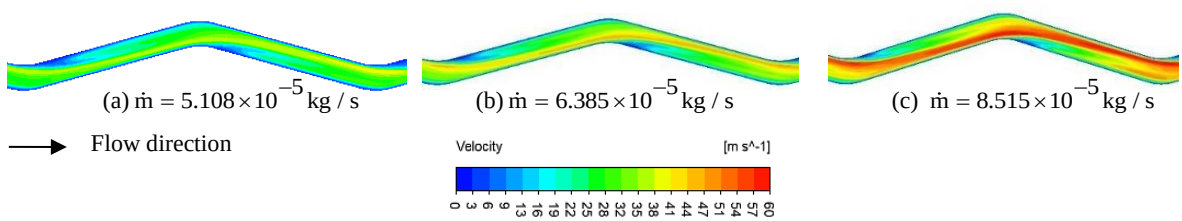

Fig. 11. Velocity magnitude distribution for Np = 8 at different mass flow rates.

As shown in Fig. 10 (a), the largest total pressure drop was found in the zigzag channel due the long length of flow channel. In addition, the zigzag channel changed the fluid flow direction at the corner, causing flow separation and vortices, increase the pressure drop. The pressure drop in the two channels increased with increasing mass flow rate owing to the increase in the fluid velocity, as shown in Fig. 11. The friction loss when the fluid passes through the channel is shown in Fig. 10 (b) using the dimensionless value of Fanning friction factor. A higher mass flow rate reduced the Fanning friction factor by about 54% in a straight channel and 36% in a zigzag channel compared to a lower mass flowrate. According to equation (7), there is an inversely proportional relationship between *f* and the mass flow rate square. However, the zigzag channel of the Fanning friction factor was predicted to be up to 45% higher than a straight channel. Figure 12(a) shows the global Nusselt number. The same trends of *h* and *Nu* increase with increasing mass flow rate owing to an increase in the channel surface heat flux. A higher global Nusselt number was observed in a zigzag channel up to 55% than in a straight channel because of the heat absorbed from the hot solid by the fluid per unit volume, resulting in an increase in the temperature on the cold side, the thermal conductivity decreasing, and *Nu* increasing.

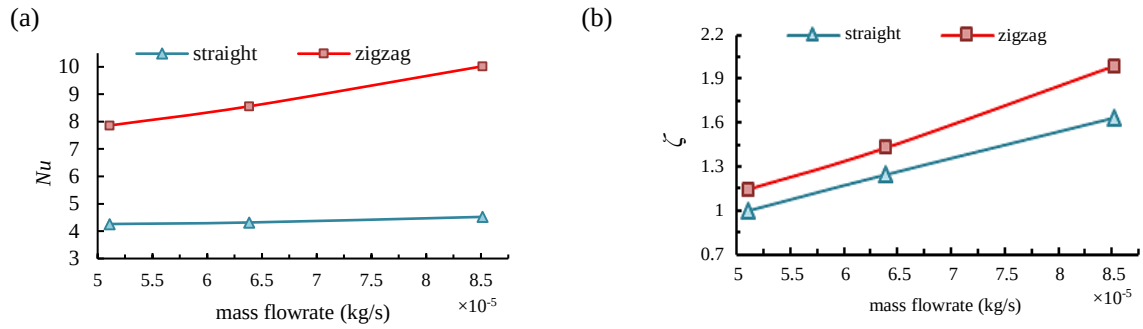

Fig. 12. (a) Global Nusselt number and (b) comprehensive performance evaluation index (ζ) at different mass flow rates for zigzag and horizontal channels.

Between straight and zigzag channel effect analysis, the simulation considered a full-length channel of 8.5 pitches with a pitch length 24.6 mm and the same cross-section area of 1.57×10^{6} m^2. However, the actual flow length was a zigzag channel of 216 mm and a straight channel of 209 mm. Therefore, the criterion $\zeta = (Nu/Nu_0)/(f/f_0)$ was applied to investigate the pressure drop and heat transfer performance for a given pumping power [7, 23-25]. Where the subscript *0* represents the comprehensive minimum performance value of the straight channel at a mass flow rate of 5.108×10^{-5} kg/s as a basis. The zigzag channel showed a higher comprehensive performance of about 16% at low mass flowrate and 22% at high mass flowrate simulation than the straight channel, as shown in Fig. 12(b). Therefore, the zigzag channel provided better heat transfer performance than flow losses.

3.3 Effect of Zigzag Channel Diameter on the PCHE Performance

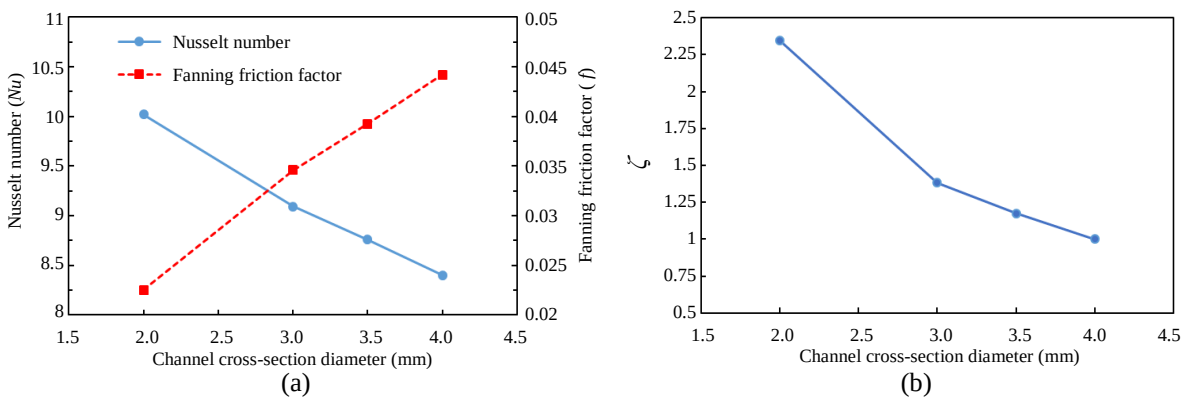

Fig. 13. Effects of channel diameter analysis (a) Global Nusselt number (*Nu*) and Fanning friction factor (*f*), and (b) comprehensive performance evaluation index (ζ) at different channel diameter (*D*).

To determine the effect of the zigzag channel diameter on PCHE performance, the same mass flow rate (8.515×10^{5} kg/s) was simulated on both sides. The channel-diameters was 2-4 mm. As shown in Fig. 13 (a), the Nusselt number decreases, and the friction factor increases more quickly with an increasing in channel diameter. This indicates that the small-diameter channel is better in terms of overall heat-transfer characteristics. In addition, the small-diameter channel reduces the friction loss, power consumption, and heat exchanger size. Therefore, the small-diameter channel exhibited a better comprehensive performance evaluation index in Fig. 13 (b).

3.4 Comparison between Present Study and Other Research of 15˚ bending Zigzag Channel

This study examines the effect of channel geometry on PCHEs performance in a laminar flow condition. Figure 14 showed that the comparison of the present study results and Kim's correlation results [17]. Kim's model used a sharp-cornered zigzag channel with a bending angle of 15˚ and a channel diameter of 1.51 mm, while the present study used

a round-cornered zigzag channel with a bending angle of 15˚ and a channel diameter of 2 mm. The round-cornered zigzag channel can provide better heat transfer. However, the present CFD study increased the Fanning friction factor. It is because the channel diameter increased by 1.32 times compared to the Kim model. This study observed a significant effects of geometrical structures and the corresponding parameters on the thermal and hydraulic performance of PCHEs. A study on the optimization of channel structure in zigzag channel PCHEs will be performed in the future.

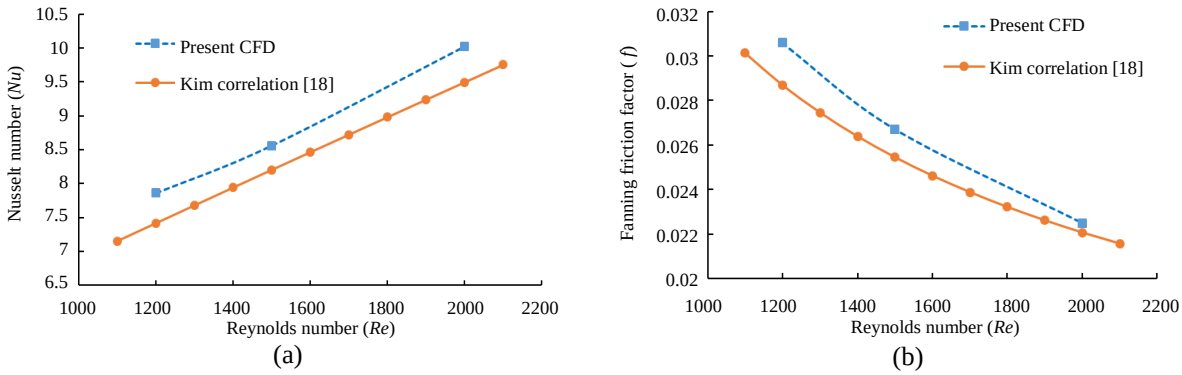

Fig. 14. Comparison of present CFD and other results (a) Nusselt number, and (b) Fanning friction factor

4. Conclusion

Two types of microchannel, straight and zigzag were investigated in this study. The effect of the thermophysical properties along the flow direction between the straight and zigzag channel PCHE was studied at a specified mass flow rate. The channel shapes were found to significantly affect the heat-hydraulic performance. In local and global analysis, the zigzag channel PCHE offered maximum heat transfer with an extra pressure drop compared to a straight channel under the considered operating regime. In addition, the global Fanning factor decreased with increasing mass flowrate, which was related to the decrease in fluid density and viscosity. The global *Nu* of all channel shapes increases with increasing mass flow rate. This study shows that a zigzag channel enhances the convective heat transfer performance and reduces the flow friction. In this study, the zigzag small-channel diameter reduced the pressure drop and increased heat transfer. Therefore, a zigzag channel with a small diameter has a relatively high comprehensive performance-evaluation index. Based on a comparative analysis, channel structures and designs with various zigzag angles are recommended.

Nomenclature

Re	Reynolds number	k	Thermal conductivity of fluid, W/mK
ΔP_f	Pressure losses, Pa	U	Fluid velocity (m/s)
A_c	Across-sectional area of channel, m^2	C_p	Specific heat J/(kg K)
l	Fluid-flow actual length, m	α	Bending channel angle, degree (˚)
$\dot{m}$	Mass flowrates, kg/s	ρ	Fluid density, kg/m^3
P	Pressure, Pa	ζ	Performance evaluation criteria
D_h	Hydraulic diameter, m	ε	Effectiveness of an heat exchanger
p	Wetted perimeter, m	g	Global
f	Pressure loss factor	w	Wall
q''	Heat flux, W/m^2	f	Fluid
h	Heat transfer coefficient, W/m^2K	h	Hot
T	Temperature, K	c	Cold
Nu	Nusselt number	i	Segment number of channel

References

[1] Takeda T, Kunitomi K, Horie T, Iwata K. Feasibility study on the applicability of a diffusion-welded compact intermediate heat exchanger to next-generation high temperature gas-cooled reactor. Nucl Eng Des. 1997;168(1-3):11-21.

[2] Natesan K, Moisseytsev A, Majumdar S. Preliminary issues associated with the next generation nuclear plant intermediate heat exchanger design. J Nucl Mater. 2009;392(2):307-315.

[3] Huang C, Cai W, Wang Y, Liu Y, Li Q, Li B. Review on the characteristics of flow and heat transfer in printed circuit heat exchangers. Appl Therm Eng. 2019;153:190-205.

[4] Chen M, Sun X, Christensen RN, Skavdahl I, Utgikar V, Sabharwall P. Dynamic behavior of a high-temperature printed circuit heat exchanger: Numerical modeling and experimental investigation. Appl Therm Eng. 2018;135:246-256.

[5] Chu WX, Li XH, Ma T, Chen YT, Wang QW. Study on hydraulic and thermal performance of printed circuit heat transfer surface with distributed airfoil fins. Appl Therm Eng. 2017;114:1309-1318.

[6] Zhao Z, Zhou Y, Ma X, Chen X, Li S, Yang S, Numerical study on thermal hydraulic performance of supercritical LNG in zigzag-type channel PCHEs. Energies. 2019;12(3):548.

[7] Pan J, Wang J, Tang L, Bai J, Li R, Lu Y, et al. Numerical investigation on thermal-hydraulic performance of a printed circuit LNG vaporizer. Appl Therm Eng. 2020;165:114447.

[8] Chu WX, Li XH, Ma T, Chen YT, Wang QW. Experimental investigation on SCO2-water heat transfer characteristics in a printed circuit heat exchanger with straight channels. Int J Heat Mass Transf. 2017;113:184-194.

[9] Zhang P, Ma T, Ke H, Wang W, Lin Y, Wang Q. Numerical investigation on local thermal characteristics of printed circuit heat exchanger for natural gas liquefication. Energy Procedia. 2019;158:5408-5413.

[10] Zhao Z, Zhou Y, Ma X, Chen X, Li S, Yang S. Effect of different zigzag channel shapes of PCHEs on heat transfer performance of supercritical LNG. Energies. 2019;12(11):2085.

[11] Yang Y, Li H, Yao M, Gao W, Zhang Y, Zhang L. Investigation on the effects of narrowed channel cross-sections on the heat transfer performance of a wavy-channeled PCHE. Int J Heat Mass Transf. 2019;135:33-43.

[12] Lee SM, Kim KY. Comparative study on performance of a zigzag printed circuit heat exchanger with various channel shapes and configurations. Heat Mass Transfer. 2013;49:1021-1028.

[13] Jeon S, Baik YJ, Byon C, Kim W. Thermal performance of heterogeneous PCHE for supercritical CO_2 energy cycle. Int J Heat Mass Transf. 2016;102:867-876.

[14] Wang Q, Xu B, Huang X, Chen Q, Wang H. Heat transfer and flow characteristics of straight-type PCHEs with rectangular channels of different widths. Nucl Eng Des. 2022;391:111734.

[15] Seung HY, Hee CN, Gil BK. Assessment of straight, zigzag, S-shape, and airfoil PCHEs for intermediate heat exchangers of HTGRs and SFRs. Nucl Eng Des. 2014;270:334-343.

[16] Chen M, Sun X, Christensen RN. Thermal-hydraulic performance of printed circuit heat exchangers with zigzag flow channels. Int J Heat Mass Transf. 2019;130:356-367.

[17] Kim IH, No HC. Thermal-hydraulic physical models for a printed circuit heat exchanger covering He, He–CO_2 mixture, and water fluids using experimental data and CFD. Exp Therm Fluid Sci. 2013;48:213-221.

[18] NIST. NIST Chemistry Webbook [Internet]. 2017 [cited 2022 Jun 15]. Available from: http://webbook.nist.gov/chemistry/.

[19] Special Metals. 2017 [cited 2022 Jul 15] Available from: https://www.specialmetals.com/documents/technical-bulletins/inconel/inconel-alloy-617.pdf.

[20] Ullah Khan MZ, Younis MY, Akram N, Akbar B, Rajput UA, Bhutta RA, et al. Investigation of heat transfer in wavy and dual wavy microchannel heat sink using alumina nanoparticles. Case Stud Therm Eng. 2021;28:101515.

[21] Hong H, Yeom E, Ji HS, Kim HD, Kim KC. Characteristics of pulsatile flows in curved stenosed channels. PLoS ONE. 2017;12(10):e0186300.

[22] Kim DE, Kim MH, Cha JE, Kim SO. Numerical investigation on thermal–hydraulic performance of new printed circuit heat exchanger model. Nucl Eng Des. 2008;238(12):3269-3276.

[23] Fan J, Yeom E. Numerical investigation on thermal hydraulic performance of supercritical LNG in PCHEs with straight, zigzag, and sinusoidal channels. J Vis. 2022;25:247-261.

[24] Wang J, Shi H, Zeng M, Ma T, Wang Q. Investigations on thermal–hydraulic performance and entropy generation characteristics of sinusoidal channeled printed circuit LNG vaporizer. Clean Technologies and Environmental Policy, 2022;24:95-108.
[25] Shi H, Raimondi NDM, Fletcher DF, Cabassud M, Gourdon C. Numerical study of heat transfer in square millimetric zigzag channels in the laminar flow regime. Chem Eng Process: Process Intensif. 2019;144:107624.